Disrupted Integration–Segregation Balance in the Intact Hemisphere in Chronic Spatial Neglect

Yusaku Takamura [1,2], Marine Lunven [3,4,5], Yvonne Serhan [6,7], Clémence Bourlon [8,9], Smadar Ovadia-Caro [6,7†], Paolo Bartolomeo [1†]

[1] Sorbonne Université, Inserm, CNRS, Paris Brain Institute, ICM, Hôpital de la Pitié-Salpêtrière, 75013 Paris, France

[2] Neurorehabilitation Research Center, Kio University, Nara, Japan

[3] Département d'Etudes Cognitives, École normale supérieure, PSL University, 75005 Paris, France

[4] University Paris Est Creteil, INSERM U955, Institut Mondor de Recherche Biomédicale, Equipe NeuroPsychologie Interventionnelle, F-94010 Créteil, France

[5] AP-HP, Hôpital Henri Mondor-Albert Chenevier, Centre de référence Maladie de Huntington, Service de Neurologie, F-94010 Créteil, France

[6] Department of Cognitive Sciences, School of Psychological Sciences, Faculty of Social Sciences,University of Haifa, Haifa, Israel.

[7] The Integrated Brain and Behavior Research Center (IBBRC), University of Haifa, Haifa, Israel

[8] Hôpitaux Paris Est Val de Marne, Soins Médicaux et de Réadaptation Neurologique, Saint Maurice, France

[9] GRC n°24 Handicap Moteur et Cognitif & Réadaptation (HaMCRe), Sorbonne Université, Assistance Publique-Hôpitaux de Paris, Paris, France

† Shared senior authorship

Paolo Bartolomeo: Sorbonne Université, Inserm, CNRS, Paris Brain Institute, ICM, Hôpital de la Pitié-Salpêtrière, 75013 Paris, France.

E-mail address: paolo.bartolomeo@icm-institute.org

Smadar Ovadia-Caro: Department of Cognitive Sciences, School of Psychological Sciences, Faculty of Social Sciences,University of Haifa, Haifa, Israel.

E-mail address: sovadiaca@cog.haifa.ac.il

Abstract

Spatial neglect is a common and disabling consequence of right hemisphere stroke, characterized by a failure to attend to the contralesional left space, and frequently persists into the chronic stage. There is robust evidence on the role of right-hemisphere frontoparietal dysfunction, interhemispheric structural disconnection and maladaptive activity in the left hemisphere in the persistence of neglect. However, the specific impact of right frontoparietal dysfunction on the functional (re)organization of the left hemisphere remains poorly understood. In this study, we introduce a novel application of functional connectivity gradient analysis to investigate macroscale functional reorganization in the non-lesioned left hemisphere of patients with chronic left spatial neglect. Focusing on resting-state fMRI data, we demonstrate that abnormal segregation patterns in the left frontoparietal and default mode networks are robustly associated with neglect severity and spatial attentional bias. Notably, the principal gradient—typically capturing a global unimodal-to-transmodal hierarchy—was altered in these patients, suggesting a reorganization favoring lateralized unimodal networks. We also show that the structural integrity of the left inferior fronto-occipital fasciculus (IFOF) plays a key role in shaping these functional dynamics. These findings reveal a previously overlooked aspect of neglect pathophysiology: the maladaptive dominance of the non-lesioned hemisphere's intrinsic architecture. By combining innovative gradient-based metrics with classical lesion approaches, our study offers a new framework for understanding neglect as an emergent property of large-scale network imbalance, with clinical implications for diagnosis and intervention, and theoretical consequences for models of hemispheric asymmetries and conscious access.

Keywords: Spatial Neglect; Functional Connectivity Gradients; Left Hemisphere Reorganization; Network Integration and Segregation; Inferior Fronto-Occipital Fasciculus (IFOF)

Highlights

- Functional connectivity gradients uncover altered segregation in the non-lesioned left hemisphere of patients with chronic spatial neglect.
- Left lateral prefrontal cortex is linked to persistent rightward attentional bias in neglect.
- Structural integrity of the left IFOF underpins functional reorganization in spared networks.
- Findings support a network-based mechanism for neglect chronicity and hemispheric asymmetry.

Abbreviations

AC: anterior commissure; AF: arcuate fasciculus; DAN: dorsal attention network; DMN: default mode network; DWI: diffusion-weighted images; FC: functional connectivity; FGs: functional connectivity gradients; FDR: false discovery rate; FPCN: frontoparietal control network; HC: healthy control; IFG: inferior frontal gyrus; IFOF: inferior fronto-occipital fasciculus; LH: left hemisphere; MFG: medial frontal gyrus; MMSE: Mini-Mental State Examination; PCA: principal component analysis; PFC: prefrontal cortex; QA: quantitative anisotropy; ROI: region of interest; SEM: standard error of the mean; SLF: superior longitudinal fasciculus; VAN: ventral attention network.

Introduction

Left spatial neglect is a disabling neuropsychological condition that frequently follows right hemisphere stroke, and is characterized by a failure to report, respond to, or orient toward stimuli presented on the contralesional side (1). In the acute phase, up to 61% of right hemisphere stroke patients present signs of contralesional neglect, compared to only 22% of those with left hemisphere damage (2). Furthermore, neglect after right-hemisphere lesions is typically more severe and persistent, with about 40% of patients exhibiting chronic symptoms months after their stroke (3). These deficits profoundly impact daily living, rehabilitation outcomes, and quality of life (4–6). Neglect is widely regarded as an attentional disorder arising from disruptions in large-scale brain networks rather than from isolated cortical lesions. Structurally, disconnections within frontoparietal networks—particularly due to damage to the superior longitudinal fasciculus (SLF)—coupled with disruption of interhemispheric callosal fibers, contribute to the onset and chronic persistence of neglect (7–10). Specifically, exploration of peripersonal space and awareness of left-sided events (11) are disrupted by damage to the ventral (12) and intermediate (13,14) branches of the right-hemisphere SLF, which connect the ventral attention network (VAN) and the dorsal attention network (DAN), respectively (15,16). Impaired interhemispheric coordination between the right and left DANs also contributes to neglect signs (15,17). Additional contributions arise from dysfunction of the default mode network (DMN), whose hyperactivity, loss of inhibition, and antagonistic interaction with the DAN are implicated in the pathophysiology and recovery of neglect (18–23).

Emerging evidence indicates that, although the lesioned right hemisphere has traditionally been the primary focus in chronic neglect, the intact left hemisphere also plays a complex and ambivalent role, acting either in a compensatory or in a maladaptive manner. Anatomical disconnection of posterior interhemispheric pathways may contribute to the

persistence of neglect (7), whereas recovery is associated with normalized interhemispheric functional connectivity, greater network segregation, and modified interactions between the DMN and attention networks in both hemispheres (15,17,22,24). In line with this hemispheric imbalance, presumably inappropriate activity in the left frontal cortex has been shown to precede left-sided omissions in chronic neglect (25). On the other hand, inhibitory neuromodulation (26) or a second stroke (27) affecting the left prefrontal cortex can instead promote neglect recovery. Altogether, this contradictory evidence highlights a complex interplay between compensatory and maladaptive plasticity, representing an important knowledge gap in understanding the evolution of neglect (28,29).

Here, we address this gap by introducing a novel approach based on functional connectivity gradients (FGs) in the non-lesioned left hemisphere of patients with chronic left neglect. Unlike traditional connectivity analyses, which focus on discrete regions or pairwise connections and may overlook the brain's global or hierarchical organization, FGs offer a low-dimensional, continuous representation of whole-brain architecture. FGs capture the spatial progression from unimodal to transmodal regions and reflects the underlying balance between functional segregation and integration—providing a powerful new lens for investigating large-scale reorganization in neglect (30,31). This approach has proven highly effective in detecting alterations across neurological and psychiatric disorders (32–35), including stroke (36). Consequently, FGs represent a promising framework for investigating distributed, macroscale brain network reorganizations related to attentional processes and their disruption in neglect chronicity (22,37).

The present study aims to identify functional signatures of disrupted integration and segregation that underlie neglect persistence and severity, and to clarify the role of the left hemisphere within large-scale cortical networks. Focusing on the chronic phase (>3 months

post-stroke) provides a valuable window largely free from transient confounds such as edema, diaschisis, and decreasing network modularity, thereby allowing a clearer interpretation of long-term network alterations (22,37–40).

Results

Participants

The data analyzed in this study were previously collected and published by Lunven et al., in a study devoted to the effects of prism adaptation in chronic neglect (8). The study received ethical approval from Inserm (C10-48) and authorization from the Ile-de-France I Ethics Committee (2011-juin-12642). All participants provided written informed consent to participate in accordance with the Declaration of Helsinki.

Here we focus on the behavioral data acquired two hours before prism adaptation. Neuroimaging data were collected before prism adaptation, depending on each participant's availability and the original study protocol (see details in Lunven et al., (8)). The dataset includes 13 patients with chronic visual neglect (Age: 63.92 ± 9.79 years, education level: 12.20 ± 2.53 years of formal education) following a right hemisphere stroke (more than 90 days post-stroke) and 10 neurologically healthy control (HC) participants matched for age and education (age: 63.4 ± 4.24 years, education level: 11.76 ± 2.99 years of formal education). Detailed demographic, clinical, and neuropsychological characteristics are presented in Table 1. Neuropsychological assessments included standardized tests commonly used to evaluate neglect sign: letter cancellation (41), copy of a linear drawing of a landscape (42), drawing from memory of a daisy (43), text reading (44), bisection of five 20-cm horizontal lines (44,45) and the landmark task (46). The neglect score (%) represents the overall severity of neglect computed using neuropsychological assessments, with higher values indicating more severe neglect (7,8). Scores were obtained according to standard procedures and conventions (see Lunven et al., (8) for a more detailed description). Lesion overlap maps for all patients and analysis pipelines are presented in Figure 1.

Table 1. Demographic and clinical characteristics of patients.

	Cutoff score	**Neglect (n = 13)** Mean (SD)
Age (years)	N/A	63.92 (9.79)
Weeks since stroke	N/A	82.68 (63.27)
Lesion volume (cm2)	N/A	200.41 (147.41)
MMSE (pts)	< 23	27 (1.92)
Neglect score (%)	N/A	31.75 (22.28)
Letter cancellation total hits (max = 60)	N/A	47.53 (12.85)
Letter cancellation L-R difference in omissions (-30 to +30)	>3	6.92 (5.79)
Gainotti drawing (max = 6)	<6	4.53 (1)
Reading (max = 116)	<116	103.15 (24.15)
Landmark "Left shorter responses"	>8	7.69 (3.24)
Line bisection (deviation mm)	>6.5	19.05 (24.27)
Daisy drawing (max = 3)	<3	1.76 (0.89)

MMSE: Mini Mental State Examination

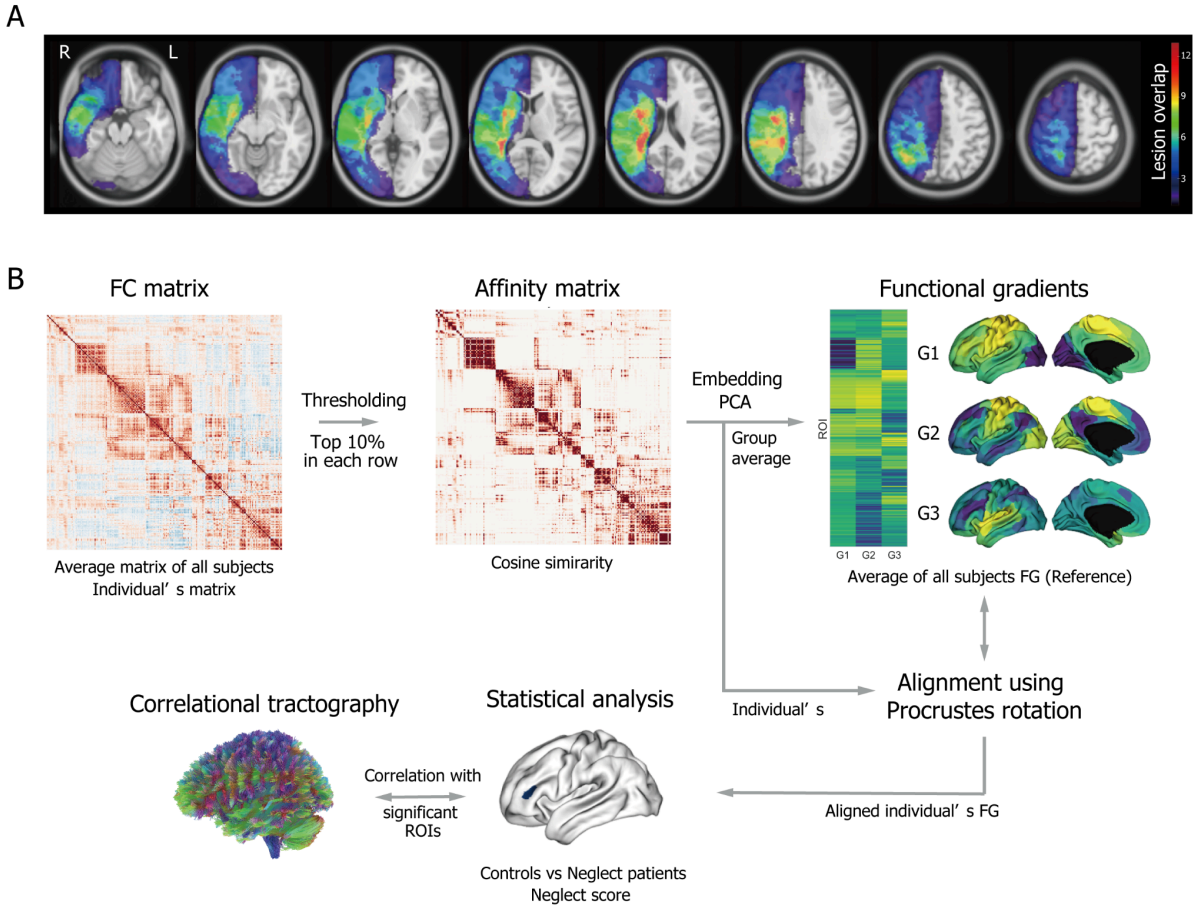

Figure 1. Lesion overlap map and schematic of the analysis pipeline.
(A) Lesion overlap map for the 13 patients included in the study. Warmer colours indicate higher overlap across individuals. (B) Overview of the analysis pipeline. Functional connectivity (FC) matrices were derived from preprocessed resting-state fMRI time series at both the group-level and individual-level. An affinity matrix was constructed by using pairwise cosine similarity for the thresholded FC matrix. Functional connectivity gradients were then extracted using principal component analysis (PCA) and projected into a low-dimensional embedding. Individual gradient maps were aligned to a group-averaged template using Procrustes alignment. Statistical comparisons were performed and regions showing significant differences were subsequently examined as the dependent variables to be explained by structural connectivity.

Spatial patterns of functional connectivity gradients

Figure 2A displays the first three FC gradients for HC and neglect patients. Together, these gradients accounted for 58.02% of the variance (23.41%, 21.11%, and 13.49%, for Gradients 1-3, respectively), with broadly similar spatial distributions across groups. Figure 2B shows pairwise scatter plots illustrating the low-dimensional embedding of cortical connectivity. Gradient 1 spanned visual to somatomotor networks, Gradient 2 extended from transmodal

regions, i.e., the DMN, to unimodal sensory networks, and Gradient 3 separated frontoparietal control network (FPCN) and DAN, from VAN and perisylvian somatomotor networks. The general arrangement of functional gradients was preserved in neglect patients, although Gradient 3 showed greater differences than Gradients 1 and 2 as indicated by the Wasserstein distance (Gradient 1: 0.042; Gradient 2: 0.065; Gradient 3: 0.142). In particular, subtle differences were observed in the dispersion of specific functional networks. Compared to HC, neglect patients showed reduced dispersion within the FPCN and DAN along Gradient 3 and increased dispersion in the DMN along Gradient 2.

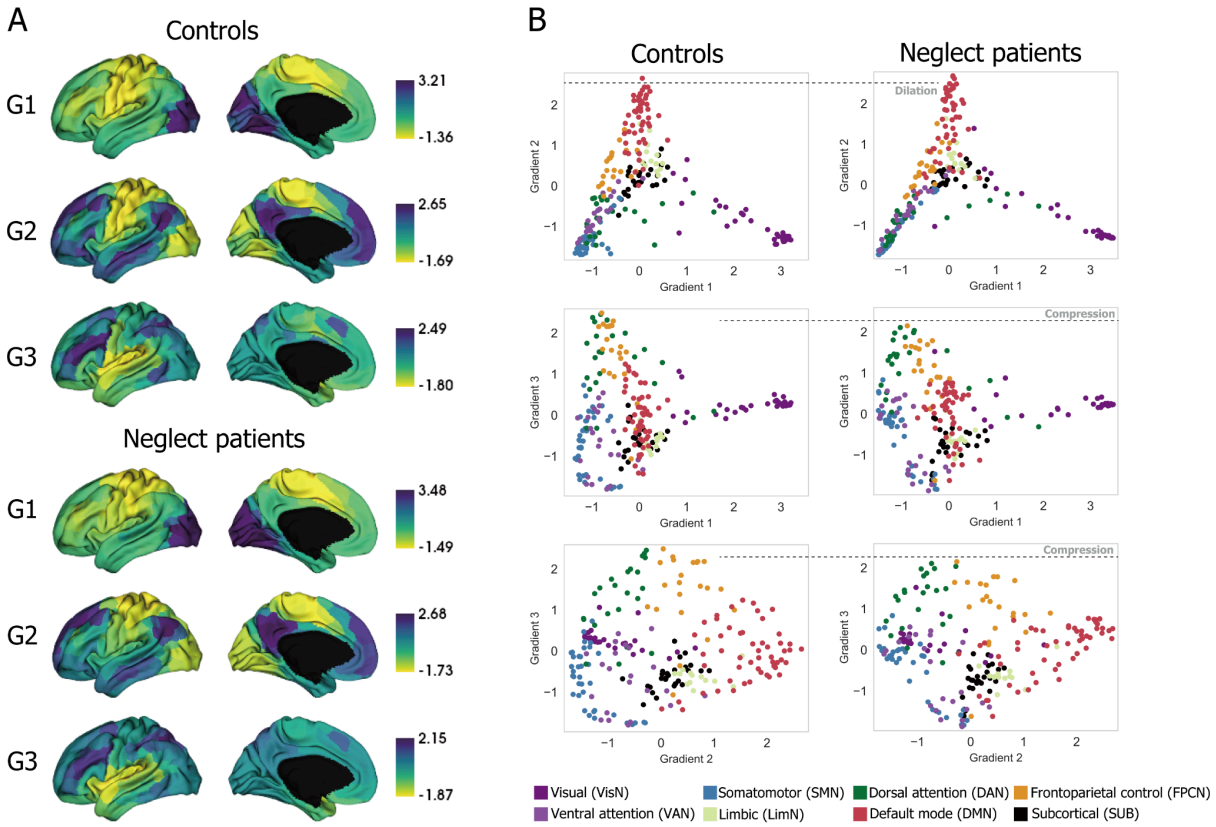

Figure 2. The general arrangement of functional networks along gradients is preserved in the left hemisphere of neglect patients and subtle differences are expressed in altered dispersion
(A) Functional connectivity gradients derived from resting-state fMRI in neglect patients and healthy controls. The top three functional gradients are shown. Gradient 1 primarily distinguishes between unimodal networks, spanning an axis from visual to somatomotor regions. Gradient 2 extends from transmodal to unimodal networks, with one extreme anchored in the default mode network and the other in sensory networks. Gradient 3 reflects task-related networks, delineating an axis from the frontoparietal control and dorsal attention networks to the ventral attention and somatomotor perisylvian networks.

(B) Pairwise scatter plots of the first three gradients highlight group-level differences, with the most prominent divergence observed in Gradient 3. Compared to healthy controls (HC), patients with neglect show reduced dispersion in regions associated with the frontoparietal control and dorsal attention networks.

Relationships between functional connectivity gradients and neglect

Figure 3 summarizes the statistical analyses of FC gradients in relation to neglect. Neglect patients showed reduced dispersion along the third Gradient in the left inferior lateral prefrontal cortex (Cont_PFCl_2) compared to HC ($t = –4.858$; pFDR = 0.0247, Figure 3A). No significant associations were found between functional gradient values and overall neglect severity scores or letter cancellation scores.

The whole-brain comparison of gradient distributions between neglect patients and HC showed significant differences in the lateral prefrontal cortex, within the frontoparietal control network in Gradient 3 (Cont_PFC1_2; pFDR<0.05, Figure 3A). Neglect patients exhibited gradient values shifted closer to zero in this region compared to controls ($t = –4.858$; $p < 0.001$; Cohen's $d = –1.832$; Figure 3B). In neglect patients, correlations between gradient values and line bisection performance revealed a negative association in the frontoparietal control network and a positive association in DMN regions (Figure 3C, pFDR<0.05). Multiple regression analysis using extracted regional gradient values, adjusted for nuisance covariates, confirmed these associations (Figure 3D; Cont_PFCl_6: $t = –5.874$; $p = 0.001$; $R^2 = 0.841$; DMN mean: $t = 11.026$; $p < 0.001$; $R^2 = 0.931$). Finally, violin plots summarized the distribution of network-level gradients (Figure 3E), highlighting a group difference in the frontoparietal control network for Gradient 3 ($t = 3.845$; pFDR = 0.00328), alongside increased dispersion in DMN in Gradient 2 in neglect patients.

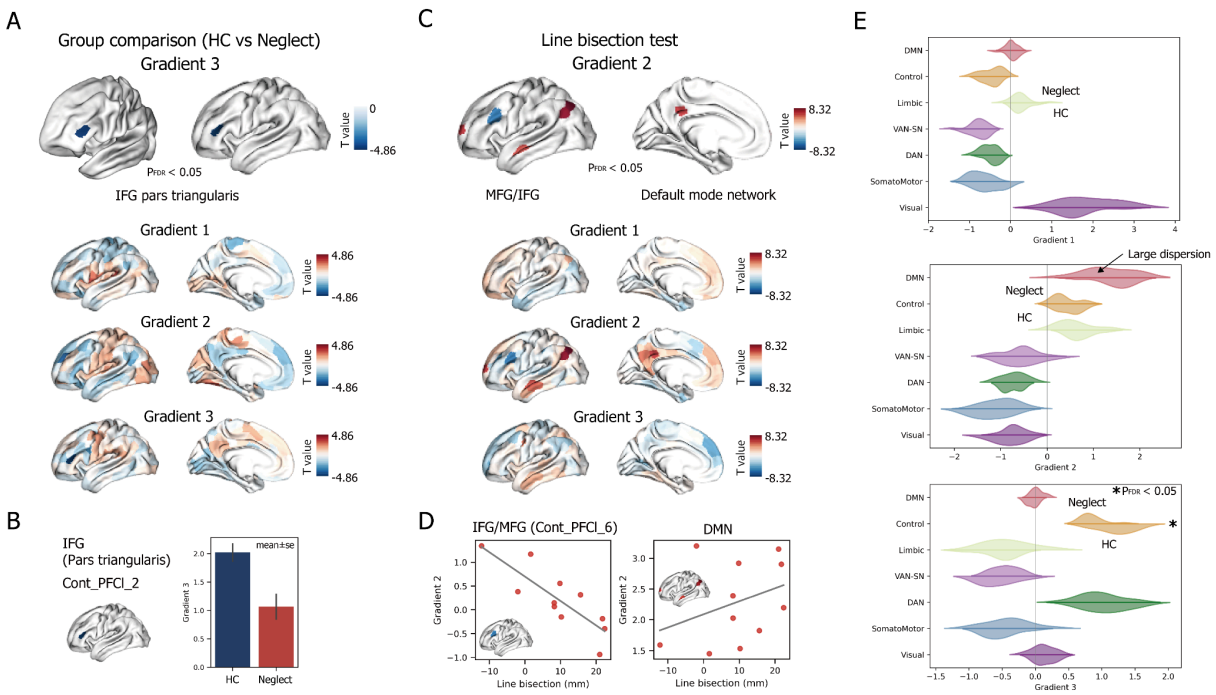

Figure 3. Areas of the frontoparietal network show reduced integration while areas of DMN show enhanced integration in neglect patients

(A) T-statistics across the three gradients comparing healthy controls (HC) and neglect patients, with statistically significant regions (pFDR < 0.05) highlighted in the top row. A significant group difference was observed in the lateral prefrontal cortex, attributed to the frontoparietal control network (Cont_PFCl_2). This region anatomically corresponds to the pars triangularis of the inferior frontal gyrus (IFG).

(B) Bar plots for Cont_PFCl_2, which showed a significant difference between the HC and neglect groups, corresponding to panels (A) and (C). Bars represent group means, and error bars indicate the standard error of the mean (SEM).

(C) T-statistics of the correlation between three gradients scores and line bisection test, with statistically significant regions (pFDR < 0.05) highlighted in the top row. A significant negative correlation was observed in the lateral prefrontal cortex, attributed to the frontoparietal control network (Cont_PFCl_6). This region anatomically corresponds to the pars triangularis of the IFG and middle frontal gyrus (MFG). Gradient 2 score at DMN also showed significant correlation with line bisection score.

(D) Correlations between neglect severity (deviation of line bisection) and gradient values in two representative regions. Left: A negative correlation was observed in the Cont_PFCl_6. Right: A positive correlation was observed in the DMN regions. Both scatter plots indicate that a greater rightward bias in line bisection was associated with gradient 2.

(E) Violin plot showing the average of three gradient networks in neglect and HC.Significant difference was observed in the frontoparietal control network in gradient 3. Large dispersion values were also observed in the default-mode network in gradient 2 (depicted by arrow).

Connectometry analysis explaining altered functional connectivity gradients

Connectometry analysis revealed a positive correlation between Gradient 3 values in the left prefrontal cortex (Cont_PFCl_2) and QA values in the anterior commissure (AC), and white

matter pathways encompassing the left occipito-temporal region, such as the inferior fronto-occipital fasciculus (IFOF), and arcuate fasciculus (AF) (Figure 4A). We observed overlap between the AC and IFOF, consistent with previous reports that their dorsoventral distributions overlap (Baudo et al., 2022). A positive correlation was also observed between the mean Gradient 2 values in DMN regions and QA values of fibers including the AF, IFOF, AC, corpus callosum, and cingulum (Figure 4A). No significant correlations were identified for Cont_PFCl_6, the region associated with line bisection deviation. To confirm the robustness of these associations, partial correlation analyses were performed between QA and functional gradient values, adjusting for lesion volume and the presence of visual field deficits. These analyses confirmed the results: Cont_PFCl_2: r = 0.568, p = 0.005, DMN mean: r = 0.544, p = 0.007 (Figure 4B)

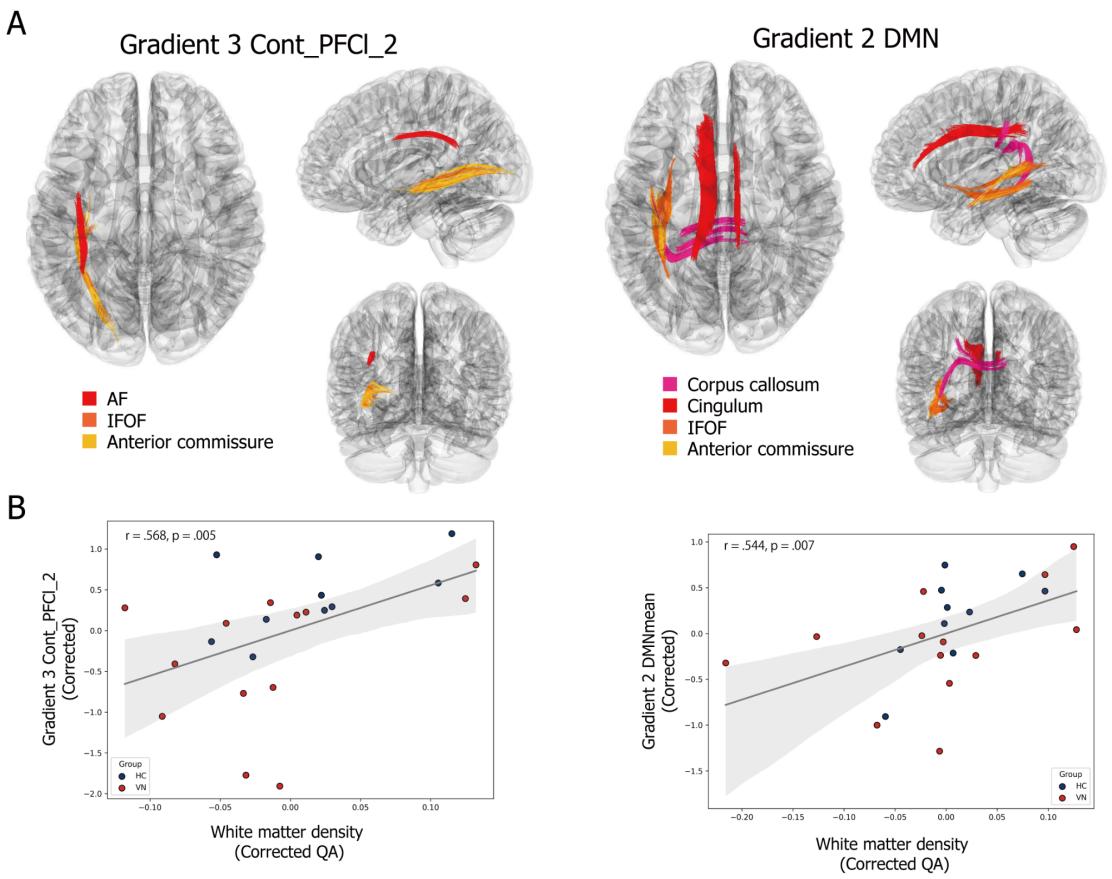

Figure 4. Changes in dispersion along the gradients are associated with underlying white matter structural integrity in both controls and patients

(A) White matter tracts linked to functional gradient alterations.
Left: WM tracts positively correlated with Cont_PFCl_2, which showed group-level differences along Gradient 3. Identified WM tracts include the arcuate fasciculus (AF), inferior fronto-occipital fasciculus (IFOF), and anterior commissure.
Right: WM tracts correlated with the default mode network (DMN), which were related to neglect severity along Gradient 2. Significant WM tracts include the corpus callosum, cingulum, IFOF, and anterior commissure.
(B) Partial correlations between white matter density (corrected QA values) and gradient scores, across both HC and neglect. Gradient scores and white matter density were corrected for nuisance variables, including lesion volume and the presence of visual deficits.

Individual analyses of functional gradients

Table 2 summarizes the differences with 95% confidence intervals between each neglect patient and the HC group in the ROI of the left lateral PFC, where a significant group difference was observed. For 11 of the 13 patients, the 95% confidence intervals did not include zero, thus showing that these patients followed the general pattern observed in the neglect group.

Table 2. The degree of deviation from the HC group in the left lateral prefrontal cortex for each neglect patient.

ID	Estimate	95%CI_low	95%CI_high	
Patient 1	-3.702	-5.471	-1.896	*
Patient 2	0.003	-0.616	0.621	
Patient 3	-0.984	-1.729	-0.202	*
Patient 4	-0.552	-1.209	0.130	
Patient 5	-0.784	-1.488	-0.057	*
Patient 6	-0.971	-1.715	-0.192	*
Patient 7	-1.900	-2.947	-0.823	*
Patient 8	-2.511	-3.795	-1.198	*

Patient 9	-4.579	-6.736	-2.401	*
Patient 10	-0.796	-1.502	-0.058	*
Patient 11	-3.195	-4.754	-1.617	*
Patient 12	-4.856	-7.131	-2.565	*
Patient 13	-0.897	-1.619	-0.138	*

* 95% confidence intervals not crossing zero.

Discussion

In this resting-state fMRI study of patients with chronic left spatial neglect, we used a novel functional gradient analysis to investigate macroscale network reorganization, focusing exclusively on the non-lesioned left hemisphere. We deliberately excluded the lesioned hemisphere considering the distributed anatomical damage in this hemisphere in the majority of patients, as well as our focus on the indirect, diascisis-like impact of the lesion on the connectome. We deliberately excluded the lesioned hemisphere, given the widespread anatomical damage in the right hemisphere in most patients and our focus on the indirect, diaschisis-like impact of the lesion on the functional connectome. By combining functional gradients, behavioral performance and structural connectivity measures, we identified altered functional segregation within key control and default mode networks, as well as structural-functional coupling involving the inferior fronto-occipital fasciculus. Our results highlight how the balance between compensatory and maladaptive mechanisms in the left hemisphere contributes to the persistence of neglect signs. These findings advance our current understanding of the neural substrates underlying chronic neglect and provide potential targets for therapeutic neuromodulation.

Reduced functional segregation in the left lateral prefrontal cortex, a key node of the frontoparietal control network, was associated with the persistence of neglect signs, as indexed by rightward deviation in the line bisection test. This observation extends and specifies convergent evidence from magnetoencephalography (25), lesion (27) and neuromodulation studies (26,48), implicating the left PFC in the pathophysiology of left neglect. In particular, Zhao et al., (48) showed that facilitatory theta burst stimulation of the left PFC improved neglect and enhanced inter-hemispheric connectivity, suggesting a possible mechanism linked to inter-hemispheric communication. This finding is consistent

with the hypothesis that the role of left-hemisphere circuits in left neglect may shift from maladaptive to compensatory, provided they can interact with lesioned right hemisphere (28,49).

Beyond its traditional association with language, the left PFC is a domain-general hub engaged in working memory, arousal, consciousness, and visual imagery (50–52). Direct stimulation of this region can elicit hallucinations (53), and neuropsychological evidence in somatoparaphrenic patients suggests that its functional dysconnection with impaired right-hemisphere networks may promote delusional misattributions of self-body (54–56). The present evidence indicates that the clinical impact of left PFC activity depends on the balance of integration and segregation within large-scale attention and control networks. On the one hand, insufficient segregation in the left PFC may diminish its ability to flexibly redistribute attentional resources. On the other hand, inappropriate hyperintegration may also be maladaptative. These disruptions of the integration–segregation balance may cause left-hemisphere perceptual decision systems (57) to receive misleading information, resulting in a lack of or inappropriate responses to left-sided events (58). Therapeutic modulation may thus act by restoring balanced segregation and interhemispheric interactions, rather than by simply increasing or decreasing activity (28).

Additionally, we found that the pathologically increased segregation of the DMN correlated with rightward attentional bias in line bisection. Because DMN activity is normally suppressed during externally oriented, attention-demanding tasks (59,60), excessive segregation of this network may reflect an intrusion of internally oriented processes (mind-wandering, self-referential mentation) that compete with external attentional control. This interpretation is supported by evidence linking DMN hyperactivity to lapses in sustained attention (18,23) and by primate stroke models in which abnormally enhanced DMN segregation is related to poorer recovery (61). Thus, our results suggest that imbalanced

DMN dynamics may limit behavioural compensatory mechanisms in chronic neglect (62–64) by interfering with attention to the external environment, although further work is required to determine whether this alteration is specific to neglect or reflects stroke severity more broadly.

Our results specify independent lines of evidence in explaining the striking hemispheric asymmetry of neglect—an unresolved question in clinical neuroscience for nearly a century (65). In the healthy brain, converging evidence from resting-state connectivity (66) and network controllability analyses (67) indicates a fundamental hemispheric asymmetry in large-scale brain organization. The left hemisphere shows a bias toward communicating within itself, supporting language and motor functions through predominantly segregated intrahemispheric interactions. In contrast, the right hemisphere exhibits a more integrative profile, engaging both intra- and interhemispheric connections—particularly with the left hemisphere. This fundamental asymmetry provides a mechanistic basis for the disproportionate impact of right-hemisphere damage on spatial and attentional functions. It further specifies the recent anatomofunctional model according to which conscious perception depends on the right hemisphere's capacity to prioritize sensory information and transmit it to left-hemisphere decision systems (58). In this view, right-hemisphere damage critically disrupts both local processing and the interhemispheric information flow necessary for awareness, thereby explaining its disproportionate impact on neglect and conscious access. The present evidence refines this model by stressing the pivotal role of the left prefrontal cortex.

In addition to the SLF, damage to a more ventral caudorostral pathway—the right-hemisphere inferior fronto-occipital fasciculus (IFOF)—has also been associated with left spatial neglect (68). Our structural-functional coupling analysis suggested a dual role of

its left-hemisphere homolog in neglect pathophysiology. Higher axonal density of the left-hemisphere IFOF was positively associated with gradient values in the left PFC (Gradient 3) and DMN (Gradient 2). This suggests that preserved structural connectivity may simultaneously contribute to compensatory reorganization within control networks while also supporting maladaptative segregation of the DMN. Similar dual contributions have been reported in motor recovery and aphasia, where the controlesional hemisphere provides both beneficial redundancy and in some cases, interference (10,69). Whether the observed correlations reflect premorbid IFOF architecture or post-stroke structural remodeling cannot be resolved in our cross-sectional design. Emerging microstructural imaging techniques and longitudinal research may clarify whether pathological changes in association tracts precede or follow functional reorganization.

In addition to the involvement of intrahemispheric pathways, previous studies underscore the critical role of the corpus callosum, the brain's largest commissural fiber bundle. The integrity of the corpus callosum facilitates interhemispheric communication, which is essential for recovery of severe forms of spatial neglect (7,8,10). Damage to the corpus callosum—particularly in its posterior segments connecting parietal regions—is associated with poorer recovery and the persistence of neglect (7), presumably because it disrupts interhemispheric interactions that support adaptive reorganization. Moreover, frontal callosal fibers may support adaptive compensatory mechanisms through communication between motor systems after prism adaptation, a visuomotor rehabilitation technique (54). Our study focused on the intact left hemisphere, thus precluding direct assessment of interhemispheric functional connectivity. However, the coupling observed between the left IFOF and DMN gradients may interact with callosal integrity to influence the degree of functional segregation or integration across hemispheres. Future studies incorporating within- and between-hemisphere structural connectivity, including detailed corpus callosum mapping,

are warranted to disentangle these relationships and better contextualize compensatory versus maladaptive mechanisms underlying neglect recovery.

Previous studies have demonstrated that changes in functional gradients are associated with disease-specific alterations in brain network architecture across neurological, psychiatric, and neurodevelopmental disorders (32–35). In particular, stroke leads to marked changes in functional connectivity gradients, especially affecting those that emphasize specific networks, rather than the networks themselves (36). This aligns with our findings, in which gradients 2 and 3 were associated with the presence and severity of neglect.

Our results highlight that plasticity after neurological disease is not limited to spontaneous reorganization of spared tissue. Rather, it reflects the interplay of residual structural pathways, compensatory recruitment, and potentially maladaptive network hyperactivity. Specifically, the left prefrontal cortex may function not only as a compensatory resource but also as a pathological reinforcer of hemispheric asymmetry, depending on the underlying connectivity dynamics. Recognizing this dual potential is critical for developing interventions. In light of recent theoretical proposals (28) and neuromodulation findings (48), strategies aimed at normalizing—rather than simply enhancing or inhibiting—left-hemisphere activity and inter-hemispheric connectivity may prove more effective.

Some limitations should be noted. First, our sample size is relatively small and lacks a control group of right hemisphere-lesioned patients without neglect; however, individual analyses confirmed the general pattern in 11 of the 13 examined patients. Second, the large lesion size introduces distortions in fMRI preprocessing, which we mitigated by focusing analyses on the intact hemisphere. While this restriction excludes interhemispheric dynamics, it also provides a novel view of reorganization in severely affected patients, who are often underrepresented in imaging studies. To advance this line of work, future research should

include longitudinal designs spanning the subacute to chronic phases of recovery (22,37), matched lesion controls without neglect, and integration with advanced neurophysiology (70,71). Such approaches will help disentangle compensatory from maladaptive mechanisms and may guide precision therapies tailored to individual connectivity profiles.

In conclusion, our study demonstrates that maladaptive plasticity—particularly involving the left lateral prefrontal cortex and default mode networks within the non-lesioned left hemisphere—contributes to the persistence of left-sided neglect symptoms in stroke survivors. Reduced functional segregation in the left prefrontal cortex as part of the frontoparietal control network and increased segregation within the DMN were both associated with persistent rightward attentional bias in the line bisection task. This may simultaneously reinforce attention to right-sided space and interfere with optimal behavioral compensation for neglect. The structural integrity of the left IFOF appears to support either compensatory or maladaptive connectivity patterns, depending on the broader brain network context, including the default mode and frontoparietal control networks. These findings highlight the distributed nature of plasticity in chronic neglect and support models that emphasize the role of maladaptive left-hemisphere functional connectivity.

Materials and Methods

Data acquisition

Patients and controls underwent MRI on a Siemens 3 T VERIO TIM system equipped with a 32-channel head coil, generating T1-weighted structural images (MPRAGE), resting-state blood oxygen level-dependent (BOLD) functional scans (rsfMRI), and diffusion-weighted images (DWI). The details of T1-weighted images, lesion mask segmentations, and DWI have been described in a previous study (8). Functional images were acquired with repetition time = 2.99s, echo time = 26 ms, flip angle = 90°, slice thickness of 3 mm, and 200 repetition times (scanning duration of approximately 10 min).

fMRI preprocessing

The data were transformed from DICOM to BIDS format using HeuDiConv (70). Next, lesion masks were included in each BIDS-style folder to reduce the warping of healthy tissue into damaged areas and vice versa during spatial normalization (71). The following description regarding the preprocessing pipeline was automatically generated by fMRIPrep. It is supported under the CC0 license. Results included in this manuscript come from preprocessing performed using fMRIPrep 24.1.1 (74), which is based on Nipype 1.8.6 (73).

Anatomical data preprocessing

Anatomical T1-weighted images were preprocessed using standard pipelines, including intensity non-uniformity correction (N4BiasFieldCorrection (76)), skull-stripping (ANTs (77)), and tissue segmentation into gray matter, white matter, and cerebrospinal fluid using FSL's FAST (78). Cortical surface reconstruction was performed with FreeSurfer's `recon-all` (79), and segmentation outputs were reconciled using Mindboggle tools (80). Spatial normalization to MNI152NLin2009cAsym and MNI152NLin6Asym standard spaces was

achieved via nonlinear registration with ANTs. Grayordinate resampling to fsLR (91k surface) was performed using Connectome Workbench tools (81). Lesion masks were included to optimize spatial normalization and minimize distortion of damaged tissue (73).

Functional data preprocessing

Functional images were preprocessed using standard pipelines. Head motion correction was performed using FSL's mcflirt (82), with motion parameters estimated relative to a reference volume generated by fMRIPrep. The BOLD reference was co-registered to the T1w image using boundary-based registration (bbregister (83)), using six degrees of freedom. Confound time series were computed, including framewise displacement (82,84), DVARS, and global signals from white matter, cerebrospinal fluid, and the whole brain. BOLD time series were mapped to the fsLR surface space using the Connectome Workbench (81), generating CIFTI-91k grayordinate files. All spatial transformations (motion correction, co-registration, normalization) were composed into a single resampling step using cubic B-spline interpolation. Subsequent preprocessing pipelines relied fMRIPrep and Nilearn v0.10.4 (85). This process included: (i) removal of the first 3 volumes to mitigate signal equilibration effects; (ii) exclusion of time points with excessive motion (>2 mm or >0.02 radians) or global signal outliers (>3 SD (86)); (iii) nuisance regression of motion parameters, white matter, cerebrospinal fluid, and global signal (19,87); and (iv) band-pass filtering (0.01–0.1 Hz (36)). Global signal regression was included to improve brain–behavior associations (88).

Functional connectivity gradients and statistical analysis

The analysis workflow is summarized in Figure 1B. Functional connectivity (FC) matrices were constructed using the Schaefer atlas (89), comprising 400 cortical parcels across 7 networks, plus 54 subcortical regions (90), for a total of 454 region of interest (ROI) Spatial

smoothing was not applied, as signal averaging within ROIs effectively reduces high-frequency noise (91). FC matrices (454 × 454) were computed using Pearson's correlation coefficient. To avoid confounds from large lesions in patients, 227 right-hemisphere ROIs were excluded, consistent with previous MEG research (25).

FC gradients were computed using Brainspace (92). The connectivity matrix was thresholded to retain the top 90% of correlation coefficients per row, and pairwise cosine similarities was calculated (36). Principal component analysis (PCA) was used for embedding, as it offers robust reliability and predictive validity for gradient mapping (93). Based on prior research, we considered selecting the top three gradients to ensure a balanced representation of connectivity patterns (36). However, to account for the restriction of our analysis to the left hemisphere only, we included up to 20 gradients. Additional components were not included when the cumulative variance explained by the first three gradients reached the levels reported in previous stroke studies (50.84% (36) and 41.63% (94)). Individual gradients were aligned to the group average using procrustes rotation (90,93,94). To compute the distance of distribution between the two groups, we also calculated the Wasserstein distance (97), after transforming the group-level gradients into z-scores, which quantifies the cost of transforming one distribution into another.

Statistical analysis was performed with Brainstat (98) using linear regression models and followed by multiple comparison correction with false discovery rate (FDR) method (99). Lesion volume and visual field deficits were included as nuisance variables (8). We compared controls and neglect patients, and examined associations between gradients and neglect severity, defined by global neglect score (7,8), line bisection deviation, and asymmetry in letter cancellation, reflecting different neglect subtypes. Two outlier neuropsychological scores were excluded for line bisection and global neglect scores defined by a two standard deviation threshold (Neglect severity: 76.03% and 81.11%; Line bisection:

73mm and 70mm). The analysis pipeline incorporated publicly available scripts and functions, including hcp-utils (https://github.com/rmldj/hcp-utils/tree/master), stroke_preprop (36) https://github.com/sheyma/stroke_preprop, and autism_gradient_asymm (100) https://github.com/wanb-psych/autism_gradient_asymm/tree/master.

Diffusion MRI preprocessing

The preprocessing pipeline has been described in a previous study (8). Subsequently, preprocessed diffusion data were processed in DSI-Studio ("Hou" version: https://dsi-studio.labsolver.org/). The following descriptions were based on the boilerplate automatically generated by DSI-Studio. It is supported under the CC BY-NC-SA 4.0 license. A total of 23 diffusion MRI scans were included in the connectometry database with the 2.000 mm in-plane resolution. The diffusion data were reconstructed in the MNI space using q-space diffeomorphic reconstruction (101) to obtain the spin distribution function (102). A diffusion sampling length ratio of 2 was used. The output resolution in diffeomorphic reconstruction was 1.72 mm isotropic. The restricted diffusion was quantified using restricted diffusion imaging (103). The tensor metrics were calculated using DWI with b-value lower than 1750 s/mm². The quantitative anisotropy (QA) was extracted as the local connectome fingerprint and used in the connectometry analysis.

Correlational tractography to explain the altered functional gradients

To understand the structural connectivity that underpins the significantly altered functional gradients, we used correlational tractography on DSIstudio (10). DSIstudio automatically generated the following descriptions. Correlational tractography (104) was derived to visualize pathways that have QA correlated with significant ROIs. A nonparametric Spearman partial correlation was used to derive the correlation, and the effect of lesion

volume and presence of visual field deficits was removed using a multiple regression model. The statistical significance of the correlation was examined using a permutation test (105). A total of 23 subjects were included in the analysis. A T-score threshold of 3.5 was assigned in the fiber tracking algorithm (104). Cerebellum was excluded. The lesion region was removed from the tracking. A seeding region was placed in the non-lesioned cerebral regions. The tracks were filtered by topology-informed pruning (105) with 16 iterations. An FDR threshold of 0.05 was applied, with 4000 randomized permutations of group labels used to estimate the null distribution of track length. Significant results were automatically segmented on DSIstudio to underlying fiber tracks.

Individual analyses of functional gradients

Neglect is often considered a heterogeneous condition, raising the possibility that patients may exhibit different patterns of resting-state brain activity. To assess potential individual differences, we conducted single-case statistical analyses comparing each neglect patient with the HC group (106–108). Singcar package (109) was used to perform the Crawford test using the Bayesian test of deficit with 100,000 iterations on R (Version 4.2.2). Statistical significance, indicating whether the neglect patients followed the group average, was assessed by testing whether the 95% confidence interval of the effect size excluded zero.

CRediT authorship contribution statement

YT: Conceptualization, Methodology, Software,Validation, Formal analysis, Data Curation,Writing - Original Draft, Writing - Review & Editing, Visualization; **ML**: Conceptualization, Methodology, Investigation, Resources, Data Curation, Writing - Review & Editing, Supervision; **YS**: Software, Writing - Review & Editing; **CB**: Investigation, Resources; **SOC**: Conceptualization, Methodology, Validation, Writing - Review & Editing, Supervision; **PB**: Conceptualization, Resources, Writing - Review & Editing, Supervision, Project administration.

Acknowledgments

During the preparation of this work, the authors used ChatGPT4 for proofreading. After using this tool, the authors reviewed and edited the content. The authors take full responsibility for the content of the publication.

Funding

The work of Y.T. is supported by the Uehara Memorial Foundation Overseas Postdoctoral Fellowship, and by JSPS KAKENHI Grants (JP24K20519 and JP24KK0296). The work of P.B. is supported by the Agence Nationale de la Recherche through ANR-16-CE37-0005 and ANR-10-IAIHU-06, by the Fondation pour la Recherche sur les AVC through FR-AVC-017, and by the Paris Brain Institute grant ViBER - Vision Beyond External Reality. The work of M.L. is supported a grant from the Agence Nationale pour la Recherche (ANR-17-EURE-0017 Frontcog, ANR-10-IDEX-0001-02 PSL*). The work of S.O.C. and Y.S. is supported by the Max-Planck partner group funding scheme, and by the Alon Scholarship for the Integration of outstanding Faculty for S.O.C from the Israeli Council for Higher Education in Israel.

References

1. Heilman KM, Valenstein E, Watson RT. Neglect and Related Disorders. Semin Neurol. 2008 Mar 19;4:209–19.

2. Cazzoli D, Kaufmann BC, Rühe H, Geiser N, Nyffeler T. Incidence of Visuospatial Neglect in Acute Stroke: Assessment and Stroke Characteristics in an Unselected 1-Year Cohort. Stroke. 2025 July;56(7):1693–703.

3. Overman MJ, Binns E, Milosevich ET, Demeyere N. Recovery of Visuospatial Neglect With Standard Treatment: A Systematic Review and Meta-Analysis. Stroke. 2024 Sept;55(9):2325–39.

4. Bosma MS, Nijboer TCW, Caljouw MAA, Achterberg WP. Impact of visuospatial neglect post-stroke on daily activities, participation and informal caregiver burden: A systematic review. Ann Phys Rehabil Med. 2020 July 1;63(4):344–58.

5. Moore MJ, Vancleef K, Riddoch MJ, Gillebert CR, Demeyere N. Recovery of Visuospatial Neglect Subtypes and Relationship to Functional Outcome Six Months After Stroke. Neurorehabil Neural Repair. 2021 Sept;35(9):823–35.

6. Oh-Park M, Hung C, Chen P, Barrett AM. Severity of Spatial Neglect During Acute Inpatient Rehabilitation Predicts Community Mobility After Stroke. PM&R. 2014 Aug 1;6(8):716–22.

7. Lunven M, Thiebaut De Schotten M, Bourlon C, Duret C, Migliaccio R, Rode G, et al. White matter lesional predictors of chronic visual neglect: a longitudinal study. Brain. 2015 Mar 1;138(3):746–60.

8. Lunven M, Rode G, Bourlon C, Duret C, Migliaccio R, Chevrillon E, et al. Anatomical predictors of successful prism adaptation in chronic visual neglect. Cortex. 2019 Nov 1;120:629–41.

9. Thiebaut de Schotten M, Tomaiuolo F, Aiello M, Merola S, Silvetti M, Lecce F, et al. Damage to white matter pathways in subacute and chronic spatial neglect: a group study and 2 single-case studies with complete virtual “in vivo” tractography dissection. Cereb Cortex N Y N 1991. 2014 Mar;24(3):691–706.

10. Kaufmann BC, Pastore-Wapp M, Bartolomeo P, Geiser N, Nyffeler T, Cazzoli D. Severity-Dependent Interhemispheric White Matter Connectivity Predicts Poststroke Neglect Recovery. J Neurosci [Internet]. 2024 May 22 [cited 2025 Jan 13];44(21). Available from: https://www.jneurosci.org/content/44/21/e1311232024

11. Martín-Signes M, Chica AB, Bartolomeo P, Thiebaut de Schotten M. Streams of conscious visual experience. Commun Biol. 2024 July 27;7(1):908.

12. Urbanski M, Thiebaut de Schotten M, Rodrigo S, Oppenheim C, Touzé E, Méder JF, et al. DTI-MR tractography of white matter damage in stroke patients with neglect. Exp Brain Res. 2011 Feb 1;208(4):491–505.

13. Thiebaut de Schotten M, Urbanski M, Duffau H, Volle E, Lévy R, Dubois B, et al. Direct evidence for a parietal-frontal pathway subserving spatial awareness in humans. Science. 2005 Sept;309(5744):2226–8.

14. Thiebaut de Schotten M, Kinkingnéhun S, Delmaire C, Lehéricy S, Duffau H, Thivard L, et al. Visualization of disconnection syndromes in humans. Cortex. 2008 Sept 1;44(8):1097–103.

15. Corbetta M, Shulman GL. Spatial neglect and attention networks. Annu Rev Neurosci. 2011;34:569–99.

16. de Schotten MT, Dell'Acqua F, Forkel SJ, Simmons A, Vergani F, Murphy DGM, et al. A lateralized brain network for visuospatial attention. Nat Neurosci. 2011 Oct;14(10):1245–6.

17. He BJ, Snyder AZ, Vincent JL, Epstein A, Shulman GL, Corbetta M. Breakdown of functional connectivity in frontoparietal networks underlies behavioral deficits in spatial neglect. Neuron. 2007 Mar;53(6):905–18.

18. Bonnelle V, Leech R, Kinnunen KM, Ham TE, Beckmann CF, Boissezon XD, et al. Default Mode Network Connectivity Predicts Sustained Attention Deficits after Traumatic Brain Injury. J Neurosci. 2011 Sept 21;31(38):13442–51.

19. Fox MD, Snyder AZ, Vincent JL, Corbetta M, Van Essen DC, Raichle ME. The human brain is intrinsically organized into dynamic, anticorrelated functional networks. Proc Natl Acad Sci U S A. 2005 July;102(27):9673–8.

20. Golland Y, Bentin S, Gelbard H, Benjamini Y, Heller R, Nir Y, et al. Extrinsic and intrinsic systems in the posterior cortex of the human brain revealed during natural sensory stimulation. Cereb Cortex N Y N 1991. 2007 Apr;17(4):766–77.

21. Raichle ME, MacLeod AM, Snyder AZ, Powers WJ, Gusnard DA, Shulman GL. A default mode of brain function. Proc Natl Acad Sci. 2001 Jan 16;98(2):676–82.

22. Ramsey LE, Siegel JS, Baldassarre A, Metcalf NV, Zinn K, Shulman GL, et al. Normalization of network connectivity in hemispatial neglect recovery. Ann Neurol. 2016;80(1):127–41.

23. Weissman DH, Roberts KC, Visscher KM, Woldorff MG. The neural bases of momentary lapses in attention. Nat Neurosci. 2006 July;9(7):971–8.

24. Umarova RM, Nitschke K, Kaller CP, Klöppel S, Beume L, Mader I, et al. Predictors and signatures of recovery from neglect in acute stroke. Ann Neurol. 2016;79(4):673–86.

25. Rastelli F, Tallon-Baudry C, Migliaccio R, Toba MN, Ducorps A, Pradat-Diehl P, et al. Neural dynamics of neglected targets in patients with right hemisphere damage. Cortex. 2013 July 1;49(7):1989–96.

26. Oliveri M, Rossini PM, Traversa R, Cicinelli P, Filippi MM, Pasqualetti P, et al. Left frontal transcranial magnetic stimulation reduces contralesional extinction in patients with unilateral right brain damage. Brain. 1999 Sept;122(9):1731–9.

27. Vuilleumier P, Hester D, Assal G, Regli F. Unilateral spatial neglect recovery after sequential strokes. Neurology. 1996 Jan;46(1):184–9.

28. Bartolomeo P. Visual neglect: getting the hemispheres to talk to each other. Brain. 2019 Apr 1;142(4):840–2.

29. Di Pino G, Pellegrino G, Assenza G, Capone F, Ferreri F, Formica D, et al. Modulation of brain plasticity in stroke: a novel model for neurorehabilitation. Nat Rev Neurol. 2014 Oct;10(10):597–608.

30. Margulies DS, Ghosh SS, Goulas A, Falkiewicz M, Huntenburg JM, Langs G, et al. Situating the default-mode network along a principal gradient of macroscale cortical organization. Proc Natl Acad Sci. 2016 Nov;113(44):12574–9.

31. Serhan Y, Darawshy S, Wei W, Margulies DS, Nenning KH, Ovadia-Caro S. Individual uniqueness of connectivity gradients is driven by the complexity of the embedded networks and their dispersion. Brain Struct Funct. 2025 July 3;230(6):110.

32. Dong D, Yao D, Wang Y, Hong SJ, Genon S, Xin F, et al. Compressed sensorimotor-to-transmodal hierarchical organization in schizophrenia. Psychol Med. 2023 Feb;53(3):771–84.

33. Hong SJ, Vos de Wael R, Bethlehem RAI, Lariviere S, Paquola C, Valk SL, et al. Atypical functional connectome hierarchy in autism. Nat Commun. 2019 Mar 4;10(1):1022.

34. Rosa APD, d'Ambrosio A, Bisecco A, Altieri M, Cirillo M, Gallo A, et al. Functional gradients reveal cortical hierarchy changes in multiple sclerosis. Hum Brain Mapp. 2024 Apr 22;45(6):e26678.

35. Tan JB, Müller EJ, Orlando IF, Taylor NL, Margulies DS, Szeto J, et al. Abnormal higher-order network interactions in Parkinson's disease visual hallucinations. Brain. 2023 Sept 7;awad305.

36. Bayrak Ş, Khalil AA, Villringer K, Fiebach JB, Villringer A, Margulies DS, et al. The impact of ischemic stroke on connectivity gradients. NeuroImage Clin. 2019 Jan 1;24:101947.

37. Siegel JS, Seitzman BA, Ramsey LE, Ortega M, Gordon EM, Dosenbach NUF, et al. Re-emergence of modular brain networks in stroke recovery. Cortex. 2018 Apr 1;101:44–59.

38. Carrera E, Tononi G. Diaschisis: past, present, future. Brain J Neurol. 2014 Sept;137(Pt 9):2408–22.

39. Grefkes C, Fink GR. Recovery from stroke: current concepts and future perspectives. Neurol Res Pract. 2020 June 16;2:17.

40. Rehme AK, Eickhoff SB, Wang LE, Fink GR, Grefkes C. Dynamic causal modeling of cortical activity from the acute to the chronic stage after stroke. NeuroImage. 2011 Apr 1;55(3):1147–58.

41. Principles of behavioral and cognitive neurology, 2nd ed. New York, NY, US: Oxford University Press; 2000. xviii, 540 p. (Mesulam MM, editor. Principles of behavioral and cognitive neurology, 2nd ed).

42. Gainotti G, D'Erme P, de Bonis C. [Clinical aspects and mechanisms of visual-spatial neglect]. Rev Neurol (Paris). 1989 Jan 1;145(8–9):626–34.

43. Rode G, Rossetti Y, Boisson D. Prism adaptation improves representational neglect. Neuropsychologia. 2001 Jan 1;39(11):1250–4.

44. Azouvi P, Bartolomeo P, Beis JM, Perennou D, Pradat-Diehl P, Rousseaux M. A battery of tests for the quantitative assessment of unilateral neglect. Restor Neurol Neurosci. 2006 Nov 1;24(4–6):273–85.

45. Urbanski M, Bartolomeo P. Line bisection in left neglect: The importance of starting right. Cortex. 2008 July 1;44(7):782–93.

46. Harvey M, Milner A d. Residual perceptual distortion in recovered hemispatial neglect. Neuropsychologia. 1999 June 1;37(6):745–50.

47. Baudo MC, Colombo EE, Pérez MA, Rahn SI, Domenech NC, Chuang J, et al. Three-Dimensional Anatomy of the Anterior Commissure: A Tractography and Anatomical Study. World Neurosurg. 2022 Mar 1;159:e365–74.

48. Zhao W, Ye L, Zhang Y, Song W, Xie H, Cao L. Potential neurophysiological mechanisms of intermittent theta-burst stimulation to the left prefrontal cortex for post-stroke unilateral neglect: An exploratory transcranial magnetic stimulation - electroencephalography study. IBRO Neurosci Rep. 2025 Dec 1;19:604–13.

49. Bartolomeo P. From competition to cooperation: Visual neglect across the hemispheres. Rev Neurol (Paris). 2021 Nov 1;177(9):1104–11.

50. Bor D, Owen AM. A common prefrontal-parietal network for mnemonic and mathematical recoding strategies within working memory. Cereb Cortex N Y N 1991. 2007 Apr;17(4):778–86.

51. Del Cul A, Dehaene S, Reyes P, Bravo E, Slachevsky A. Causal role of prefrontal cortex in the threshold for access to consciousness. Brain. 2009 Sept 1;132(9):2531–40.

52. Dijkstra N, Rein T von, Kok P, Fleming SM. A neural basis for distinguishing imagination from reality. Neuron [Internet]. 2025 June 5 [cited 2025 June 14];0(0). Available from: https://www.cell.com/neuron/abstract/S0896-6273(25)00362-9

53. Blanke O, Landis T, Seeck M. Electrical cortical stimulation of the human prefrontal cortex evokes complex visual hallucinations. Epilepsy Behav EB. 2000 Oct;1(5):356–61.

54. Bartolomeo P, de Vito S, Seidel Malkinson T. Space-related confabulations after right hemisphere damage. Cortex. 2017 Feb 1;87:166–73.

55. Halligan PW, Marshall JC, Wade DT. Unilateral Somatoparaphrenia After Right Hemisphere Stroke: A Case Description. Cortex. 1995 Mar 1;31(1):173–82.

56. Saetta G, Michels L, Brugger P. Where in the Brain is “the Other’s” Hand? Mapping Dysfunctional Neural Networks in Somatoparaphrenia. Neuroscience. 2021 Nov 10;476:21–33.

57. Heekeren HR, Marrett S, Bandettini PA, Ungerleider LG. A general mechanism for perceptual decision-making in the human brain. Nature. 2004 Oct;431(7010):859–62.

58. Bartolomeo P, Liu J, Seidel Malkinson T. Frontoparietal asymmetries leading to conscious perception. Trends Cogn Sci. 2025 Mar;29(3):222–5.

59. Broyd SJ, Demanuele C, Debener S, Helps SK, James CJ, Sonuga-Barke EJS. Default-mode brain dysfunction in mental disorders: A systematic review. Neurosci Biobehav Rev. 2009 Mar 1;33(3):279–96.

60. Menon V. 20 years of the default mode network: a review and synthesis. Neuron. 2023 Aug 16;111(16):2469–87.

61. Nashed JY, Gale DJ, Gallivan JP, Cook DJ. Changes in cortical manifold structure following stroke and its relation to behavioral recovery in the male macaque. Nat Commun. 2024 Oct 18;15(1):9005.

62. Bartolomeo P. The Novelty Effect in Recovered Hemineglect. Cortex. 1997 Jan 1;33(2):323–33.

63. Takamura Y, Imanishi M, Osaka M, Ohmatsu S, Tominaga T, Yamanaka K, et al. Intentional gaze shift to neglected space: a compensatory strategy during recovery after unilateral spatial neglect. Brain. 2016;139(11):2970–82.

64. Tham K, Borell L, Gustavsson A. The Discovery of Disability: A Phenomenological Study of Unilateral Neglect. Am J Occup Ther. 2000 July 1;54(4):398–406.

65. BRAIN WR. VISUAL DISORIENTATION WITH SPECIAL REFERENCE TO LESIONS OF THE RIGHT CEREBRAL HEMISPHERE. Brain. 1941 Dec 1;64(4):244–72.

66. Gotts SJ, Jo HJ, Wallace GL, Saad ZS, Cox RW, Martin A. Two distinct forms of functional lateralization in the human brain. Proc Natl Acad Sci. 2013 Sept 3;110(36):E3435–44.

67. Ben Messaoud R, Le Du V, Bousfiha C, Corsi MC, Gonzalez-Astudillo J, Kaufmann BC, et al. Low-dimensional controllability of brain networks. PLoS Comput Biol. 2025 Jan;21(1):e1012691.

68. Urbanski M, Thiebaut De Schotten M, Rodrigo S, Catani M, Oppenheim C, Touzé E, et al. Brain networks of spatial awareness: evidence from diffusion tensor imaging tractography. J Neurol Neurosurg Psychiatry. 2008 May;79(5):598–601.

69. Saur D, Lange R, Baumgaertner A, Schraknepper V, Willmes K, Rijntjes M, et al. Dynamics of language reorganization after stroke. Brain. 2006 June 1;129(6):1371–84.

70. Chea M, Ben Salah A, Toba MN, Zeineldin R, Kaufmann B, Weill-Chounlamountry A, et al. Listening to classical music influences brain connectivity in post-stroke aphasia: A pilot study. Ann Phys Rehabil Med. 2024 May;67(4):101825.

71. Massimini M, Corbetta M, Sanchez-Vives MV, Andrillon T, Deco G, Rosanova M, et al. Sleep-like cortical dynamics during wakefulness and their network effects following brain injury. Nat Commun. 2024 Aug 22;15(1):7207.

72. Halchenko YO, Goncalves M, Ghosh S, Velasco P, Castello MV di O, Salo T, et al. HeuDiConv — flexible DICOM conversion into structured directory layouts. J Open Source Softw. 2024 July 3;9(99):5839.

73. Brett M, Leff AP, Rorden C, Ashburner J. Spatial Normalization of Brain Images with Focal Lesions Using Cost Function Masking. NeuroImage. 2001 Aug 1;14(2):486–500.

74. Esteban O, Markiewicz CJ, Blair RW, Moodie CA, Isik AI, Erramuzpe A, et al. fMRIPrep: a robust preprocessing pipeline for functional MRI. Nat Methods. 2019 Jan;16(1):111–6.

75. Gorgolewski KJ, Auer T, Calhoun VD, Craddock RC, Das S, Duff EP, et al. The brain imaging data structure, a format for organizing and describing outputs of neuroimaging experiments. Sci Data. 2016 June 21;3(1):160044.

76. Tustison NJ, Avants BB, Cook PA, Zheng Y, Egan A, Yushkevich PA, et al. N4ITK: improved N3 bias correction. IEEE Trans Med Imaging. 2010 June;29(6):1310–20.

77. Avants BB, Epstein CL, Grossman M, Gee JC. Symmetric diffeomorphic image registration with cross-correlation: evaluating automated labeling of elderly and neurodegenerative brain. Med Image Anal. 2008 Feb;12(1):26–41.

78. Zhang Y, Brady M, Smith S. Segmentation of brain MR images through a hidden Markov random field model and the expectation-maximization algorithm. IEEE Trans Med Imaging. 2001 Jan;20(1):45–57.

79. Dale AM, Fischl B, Sereno MI. Cortical surface-based analysis. I. Segmentation and surface reconstruction. NeuroImage. 1999 Feb;9(2):179–94.

80. Klein A, Ghosh SS, Bao FS, Giard J, Häme Y, Stavsky E, et al. Mindboggling morphometry of human brains. PLOS Comput Biol. 2017 Feb 23;13(2):e1005350.

81. Glasser MF, Sotiropoulos SN, Wilson JA, Coalson TS, Fischl B, Andersson JL, et al. The minimal preprocessing pipelines for the Human Connectome Project. NeuroImage. 2013 Oct;80:105–24.

82. Jenkinson M, Bannister P, Brady M, Smith S. Improved optimization for the robust and accurate linear registration and motion correction of brain images. NeuroImage. 2002 Oct;17(2):825–41.

83. Greve DN, Fischl B. Accurate and robust brain image alignment using boundary-based registration. NeuroImage. 2009 Oct;48(1):63–72.

84. Power JD, Mitra A, Laumann TO, Snyder AZ, Schlaggar BL, Petersen SE. Methods to detect, characterize, and remove motion artifact in resting state fMRI. NeuroImage. 2014 Jan;84:320–41.

85. Abraham A, Pedregosa F, Eickenberg M, Gervais P, Mueller A, Kossaifi J, et al. Machine learning for neuroimaging with scikit-learn. Front Neuroinformatics [Internet]. 2014 Feb 21 [cited 2025 Oct 15];8. Available from: https://www.frontiersin.org/journals/neuroinformatics/articles/10.3389/fninf.2014.00014/full

86. Demertzi A, Tagliazucchi E, Dehaene S, Deco G, Barttfeld P, Raimondo F, et al. Human consciousness is supported by dynamic complex patterns of brain signal coordination. Sci Adv. 2019 Feb 6;5(2):eaat7603.

87. Wang HT, Meisler SL, Sharmarke H, Clarke N, Gensollen N, Markiewicz CJ, et al. Continuous evaluation of denoising strategies in resting-state fMRI connectivity using fMRIPrep and Nilearn. PLOS Comput Biol. 2024 Mar 18;20(3):e1011942.

88. Li J, Kong R, Liégeois R, Orban C, Tan Y, Sun N, et al. Global signal regression strengthens association between resting-state functional connectivity and behavior. NeuroImage. 2019 Aug;196:126–41.

89. Schaefer A, Kong R, Gordon EM, Laumann TO, Zuo XN, Holmes AJ, et al. Local-Global Parcellation of the Human Cerebral Cortex from Intrinsic Functional Connectivity MRI. Cereb Cortex N Y N 1991. 2018 Sept;28(9):3095–114.

90. Tian Y, Margulies DS, Breakspear M, Zalesky A. Topographic organization of the human subcortex unveiled with functional connectivity gradients. Nat Neurosci. 2020 Nov;23(11):1421–32.

91. Alakörkkö T, Saarimäki H, Glerean E, Saramäki J, Korhonen O. Effects of spatial smoothing on functional brain networks. Eur J Neurosci. 2017;46(9):2471–80.

92. Vos de Wael R, Benkarim O, Paquola C, Lariviere S, Royer J, Tavakol S, et al. BrainSpace: a toolbox for the analysis of macroscale gradients in neuroimaging and connectomics datasets. Commun Biol. 2020 Mar 5;3(1):1–10.

93. Hong SJ, Xu T, Nikolaidis A, Smallwood J, Margulies DS, Bernhardt B, et al. Toward a connectivity gradient-based framework for reproducible biomarker discovery. NeuroImage. 2020 Dec 1;223:117322.

94. Koba C, Falcó-Roget J, Crimi A. Reshaped functional connectivity gradients in acute ischemic stroke. NeuroImage Clin. 2025;45:103755.

95. Kim S, Yoo S, Xie K, Royer J, Larivière S, Byeon K, et al. Comparison of different group-level templates in gradient-based multimodal connectivity analysis. Netw Neurosci. 2024 Oct 22;1–23.

96. Langs G, Golland P, Ghosh SS. Predicting Activation Across Individuals with Resting-State Functional Connectivity Based Multi-Atlas Label Fusion. Med Image Comput Comput-Assist Interv MICCAI Int Conf Med Image Comput Comput-Assist Interv. 2015 Oct;9350:313–20.

97. Ramdas A, Trillos NG, Cuturi M. On Wasserstein Two-Sample Testing and Related Families of Nonparametric Tests. Entropy. 2017 Feb;19(2):47.

98. Larivière S, Bayrak Ş, Vos de Wael R, Benkarim O, Herholz P, Rodriguez-Cruces R, et al. BrainStat: A toolbox for brain-wide statistics and multimodal feature associations. NeuroImage. 2023 Feb 1;266:119807.

99. Benjamini Y, Hochberg Y. Controlling the False Discovery Rate: A Practical and Powerful Approach to Multiple Testing. J R Stat Soc Ser B Methodol. 1995;57(1):289–300.

100. Wan B, Hong SJ, Bethlehem RAI, Floris DL, Bernhardt BC, Valk SL. Diverging asymmetry of intrinsic functional organization in autism. Mol Psychiatry. 2023 Oct;28(10):4331–41.

101. Yeh FC, Tseng WYI. NTU-90: a high angular resolution brain atlas constructed by q-space diffeomorphic reconstruction. NeuroImage. 2011 Sept;58(1):91–9.

102. Yeh FC, Wedeen VJ, Tseng WYI. Generalized q-sampling imaging. IEEE Trans Med Imaging. 2010 Sept;29(9):1626–35.

103. Yeh FC, Liu L, Hitchens TK, Wu YL. Mapping immune cell infiltration using restricted diffusion MRI. Magn Reson Med. 2017 Feb;77(2):603–12.

104. Yeh FC, Irimia A, Bastos DC de A, Golby AJ. Tractography methods and findings in brain tumors and traumatic brain injury. NeuroImage. 2021 Dec;245:118651.

105. Yeh FC, Badre D, Verstynen T. Connectometry: A statistical approach harnessing the analytical potential of the local connectome. NeuroImage. 2016 Jan;125:162–71.

106. Yeh FC, Verstynen TD, Wang Y, Fernández-Miranda JC, Tseng WYI. Deterministic Diffusion Fiber Tracking Improved by Quantitative Anisotropy. PLOS ONE. 2013 Nov 15;8(11):e80713.

107. Yeh FC, Panesar S, Barrios J, Fernandes D, Abhinav K, Meola A, et al. Automatic Removal of False Connections in Diffusion MRI Tractography Using Topology-Informed Pruning (TIP). Neurother J Am Soc Exp Neurother. 2019 Jan;16(1):52–8.

108. Crawford JR, Garthwaite PH, Howell DC. On comparing a single case with a control sample: an alternative perspective. Neuropsychologia. 2009 Nov;47(13):2690–5.

109. Crawford JR, Garthwaite PH, Porter S. Point and interval estimates of effect sizes for the case-controls design in neuropsychology: rationale, methods, implementations, and proposed reporting standards. Cogn Neuropsychol. 2010 May;27(3):245–60.

110. Cubelli R, Della Sala S. Looking back to go forward: Promoting single case studies. Cortex. 2017 Dec 1;97:A1–3.

111. Rittmo J, McIntosh RD. singcar: Comparing single cases to small samples in R. J Open Source Softw. 2021 Dec 30;6(68):3887.